Dissipative chaos in semiconductor superlattices

Kirill N. Alekseev and Gennady P. Berman
Center for Nonlinear Studies and Theoretical Division, Los Alamos National Laboratory, Los Alamos, New Mexico 87545;
Kirensky Institute of Physics, 660036, Krasnoyarsk, Russia;
and Department of Physics, University of Illinois at Urbana-Champaign, 1110 West Green Street, Urbana, Illinois 61801-3080

David K. Campbell, Ethan H. Cannon, and Matthew C. Cargo
Department of Physics, University of Illinois at Urbana-Champaign, 1110 West Green Street, Urbana, Illinois 61801-3080
(Received 30 April 1996)

We consider the motion of ballistic electrons in a miniband of a semiconductor superlattice (SSL) under the influence of an external, time-periodic electric field. We use a semiclassical, balance-equation approach, which incorporates elastic and inelastic scattering (as dissipation) and the self-consistent field generated by the electron motion. The coupling of electrons in the miniband to the self-consistent field produces a cooperative nonlinear oscillatory mode which, when interacting with the oscillatory external field and the intrinsic Bloch-type oscillatory mode, can lead to complicated dynamics, including dissipative chaos. For a range of values of the dissipation parameters we determine the regions in the amplitude-frequency plane of the external field in which chaos can occur. Our results suggest that for terahertz external fields of the amplitudes achieved by present-day free-electron lasers, chaos may be observable in SSL's. We clarify the nature of this interesting nonlinear dynamics in the superlattice–external-field system by exploring analogies to the Dicke model of an ensemble of two-level atoms coupled with a resonant cavity field, and to Josephson junctions. [S0163-1829(96)05440-9]

I. INTRODUCTION

More than two decades ago, Esaki and Tsu[1] discovered a striking nonlinear effect in semiconductor superlattices (SSL's), establishing that the dissipative motion of electrons within a single SSL miniband in the presence of a *static* electric field can produce a *negative differential conductivity* (NDC) in the stationary current-voltage characteristic. In view of its potential applications to ultrasmall electronic devices,[2] interest in this effect remains high,[3] and it continues to be studied by a variety of different theoretical and experimental techniques.[4,5] The importance of these systems is reflected, for example, in the many articles in semipopular physics literature.[6]

In the past several years, technological advances in semiconductor nanostructure fabrication and in electromagnetic field generation techniques have made possible detailed studies of a wide range of other nonlinear phenomena involving electron transport in SSL's in the presence of a variety of electromagnetic (EM) fields.[4,5] Very recently, the effect of alternating fields in the terahertz (THz) domain on the nonlinear current-voltage characteristics of superlattices has been investigated experimentally,[7] and observations of photon-assisted resonant tunneling and negative *absolute* resistance have been reported.[8]

These extensive experimental efforts have been paralleled by many related theoretical studies.[9–17] These studies have examined the propagation of the electromagnetic solitons through the superlattice,[9] self-consistent nonlinear plasma oscillations,[10–12] Hamiltonian chaotic dynamics of electrons in a constant magnetic field interacting with electromagnetic waves,[13] and emission of electromagnetic radiation from superlattices due to multiphoton transitions.[14] Although most of these studies have been in the semiclassical regime, the consequences of a fully quantum-mechanical treatment of miniband transport in an intense oscillating EM field have also been examined.[15] Reviews of these and other theoretical studies are given in Refs. 16 and 17. All these investigations have dealt with the *intraminiband* dynamics of the electron, neglecting the possibility of *interminiband* transitions; additional nonlinear phenomena can become relevant if interminiband dynamics are considered.

In a previous paper,[18] we extended earlier studies of the *intraminiband* dynamics of ballistic electrons in a SSL with an ac external electric field by taking into account the self-consistent EM field generated by the electron current. The coupling of the electron motion to the self-consistent field results in cooperative oscillations which alter the dynamics substantially. In particular, we showed that, with the inclusion of the self-consistent field, the inherently nonlinear nature of the electron dynamics implies that, under the influence of the external ac field, various dynamical instabilities, including transitions to chaos, can occur.[18] However, our previous work was limited to the *nondissipative* regime and thus was strictly valid only on time scales shorter than all characteristic relaxation times for the electron's energy and momentum. Hence, *a priori* we could not determine the long-time (stationary) dynamical behavior. More importantly, the assumption of no dissipation is of dubious applicability to the interpretation of experiments in real systems, in which dissipative effects are certainly present at some level.

In the present study, we generalize our previous work by considering explicitly the role of dissipation in the balance equations describing the SSL plus field system. After recalling briefly how the conventional balance equations recover

the standard results of Bloch oscillations and negative differential conductivity, we show that our extension of the balance equations to account for collective effects on the electron's motion can (for certain conditions) result in chaotic dynamics, both transient and stationary, even in the presence of damping. We discuss and exploit analogies between the electrons in a SSL plus field system, and the dynamics of lasers and optical bistable systems and of damped, driven Josephson junctions; the extensive tradition of studying dissipative nonlinear dynamics in these problems allows us to use these analogies to guide our studies of the semiconductor system.

The remainder of the paper is organized into three sections. In Sec. II we use a balance equation approach to formulate (phenomenological) equations of the motion for the electron in the SSL in the presence of an external ac field, including the self-consistent field generated by the electron current. We show how to incorporate various dissipative channels in these equations, and illustrate that the solutions to these equations capture the anticipated behavior in several simple limiting cases, including those of (undamped) Bloch oscillations and (stationary) negative differential conductivity. In preparation for our study of the general case, we introduce a rescaled (pseudospin) representation of the equations of motion, and demonstrate the analogy with the optical systems, in which chaotic behavior is well established. In Sec. III we present the details of our study of the dissipative chaotic dynamics of the SSL plus field system. First, we show that our equations reduce (in two different limits) to the equations of two well-known chaotic systems, (1) the Lorenz equations and (2) the damped, driven pendulum. Second, we present numerical studies of the full equations. Our results suggest that, for a wide range of values of the frequency and amplitude of the external field and for experimentally relevant values of the damping, stationary chaotic dynamics should be observed, interspersed with transient chaos, leading eventually to periodic motion. We provide detailed confirmation of the chaotic behavior in the form of Lyapunov exponents, power spectra, and direct time evolution traces. In Sec. IV we summarize our results, examine critically the possible parameter ranges in which the effects we predict can be observed in experiments, discuss how these effects might manifest themselves in experimental observables, and mention a number of open theoretical issues.

II. BALANCE EQUATION APPROACH

Consider the motion of ballistic electrons in a SSL in the presence of an external ac electric field with amplitude E_0 and frequency Ω,

$$E_{\rm ext}(t)=E_0\cos\Omega t, \tag{1}$$

which is applied in the direction perpendicular to the layers of the SSL, i.e., in the direction of the motion within the SSL miniband. In the standard tight-binding approximation, the dispersion relation of the electron belonging to a single miniband in the SSL is[1,16]

$$\varepsilon(p)=\frac{\Delta}{2}\left[1-\cos\left(\frac{pa}{\hbar}\right)\right], \tag{2}$$

where Δ is the miniband width, and a is the SSL periodicity. This nonquadratic dependence of the electron energy on the quasimomentum within the miniband renders the dynamics of electrons inherently nonlinear.

Generalizing the balance equation approach of Ref. 14 to incorporate the self-consistent field[19,20] generated by the electron current, we find that (with the assumption of spatial homogeneity) the equations describing the electron's motion in the combined external and self-consistent field become

$$\dot V=-eE_{\rm tot}(t)/m(\varepsilon)-\gamma_v V, \tag{3a}$$

$$\dot\varepsilon=-eE_{\rm tot}(t)V-\gamma_\varepsilon(\varepsilon-\varepsilon_0), \tag{3b}$$

$$\dot E_{sc}=-4\pi j-\alpha E_{\rm sc}, \tag{3c}$$

where

$$E_{\rm tot}(t)=E_{\rm sc}(t)+E_{\rm ext}(t)\quad\text{and}\quad j\equiv -eNV. \tag{3d}$$

In Eqs. (3), V is the average velocity (along the SSL axis), and N is the number of electrons per unit volume, so that j is the average electron current density, ε is the average energy of the electrons, ε_0 is the equilibrium energy of carriers (resulting from thermal energy and/or external pumping), and $E_{\rm sc}$ is the self-consistent EM field generated by the electron current j. All quantities are measured in cgs units.

Let us say a few words about the physical interpretation of these equations. Equation (3a) is the basic equation of motion of electrons belonging to one miniband [with the dispersion law (2)] in the presence of the electric field $E_{\rm tot}(t)$. Importantly, the dependence of the electron's effective mass $m(\varepsilon)$ on energy in Eq. (3a) is[14]

$$m(\varepsilon)=\frac{m_0}{1-2\varepsilon/\Delta},\quad m_0\equiv\frac{2\hbar^2}{\Delta a^2}, \tag{4}$$

where m_0 is the electron's effective mass at the bottom of the miniband. Note that $m(\varepsilon)$ may take negative values for $\varepsilon>\Delta/2$. The occurrence of a negative effective mass is connected with the existence of negative differential drift velocities (see, e.g., Ref. 14 and references therein).

Equation (3b) describes the heating (i.e., increase in energy) of the electrons by the field $E_{\rm tot}(t)$ and cooling (i.e., relaxation of energy) to the equilibrium value ε_0. The thermal equilibrium energy value ε_0 has the temperature dependence[14,21]

$$\varepsilon_0^{(T)}=\frac{\Delta}{2}\left[1-\frac{I_1(\Delta/2k_BT)}{I_0(\Delta/2k_BT)}\right], \tag{5}$$

where $I_{0,1}$ are the modified Bessel functions, T is the lattice temperature, and k_B is Boltzmann's constant.

The parameters γ_v, γ_ε, and α are the *phenomenological* relaxation constants of the average velocity, energy, and self-consistent field, respectively. The treatment of these relaxation parameters as constants, independent of energy, is an approximation; we shall discuss our present understanding of the validity of this approximation in Sec. IV. Physically, in a SSL, the damping of the average velocity is mainly due to the elastic scattering of electrons with the impurities, struc-

tural disorder, and interface roughness. Typically, the main channel of energy dissipation for the electron subsystem is inelastic phonon scattering.

Equation (3c) is Maxwell's equation for the time evolution of the self-consistent electric field, with an additional term describing its relaxation. The form of this equation, including the phenomenological relaxation constant, α — which models effects of interactions of the self-consistent field with degrees of freedom beyond the ballistic electrons described dynamically in our equations — is familiar from the literature on bulk semiconductors.[19] Examples of the processes contributing to α include surface effects and the generation of polar phonons due to the finite polarization of the crystal produced by the field.

Following the original deviations of the ''balance equations'' (3a) and (3b) in Refs. 22 and 23, several articles have discussed the *microscopic* derivation and justification of the equations and their use in modeling both general transport properties in SSLs (Ref. 24) and specific nanoscale devices.[2,25] For our present purposes, however, it is sufficient to consider Eqs. (3) as a phenomenological set of equations.

Before analyzing the nonlinear dynamics of the full system (3) in detail, let us examine briefly several important limiting cases, in order to illustrate the consistency of the balance equation approach with known results. For simplicity, we shall momentarily ignore the self-consistent field equation entirely and focus on the consequences of Eqs. (3a) and (3b) alone. Consider first the case in which the electrons in the SSL are influenced only by a *constant* external field $E_{\rm tot}=E_{\rm ext}=E_0=\text{const}$, and for which the relaxation processes can be neglected: i.e., $\gamma_\varepsilon=\gamma_v=0$. In this simple limiting case, a straightforward calculation shows that the electrons perform harmonic oscillations with velocity $V=V_0\sin\omega_s t$. These are the familiar Bloch oscillations,[1,6] and the characteristic frequency of these oscillations $\omega_s=eaE_0/\hbar$ is known as the Bloch[7] or Stark[16] frequency. For typical SSL's and for typical electric fields, ($\sim$1–10 kV/cm), the Bloch frequency belongs to the THz domain. Although there remains some controversy, experimental evidence for these Bloch oscillations has recently been reported.[26]

Consider next the case in which there is still a constant electric field and the relaxation effects are also included, so that $\gamma_v\neq 0$, $\gamma_\varepsilon\neq 0$. This problem was first considered by Esaki and Tsu[1] for the particular case $\gamma_v=\gamma_\varepsilon$, and the generalization to the case $\gamma_v\neq\gamma_\varepsilon$ is given in Refs. 14, 22, and 23. Again, a straightforward calculation shows that the system undergoes damped oscillations and that in the steady state the current $j=-eNV$ becomes

$$j=\frac{e^2NE_0/\gamma_v}{1+((eE_0a/\hbar)^2/(\gamma_v\gamma_\varepsilon))}\,\frac{I_1(\Delta/2k_BT)}{I_0(\Delta/2k_BT)}\,\frac{1}{m_0}, \tag{6}$$

which reduces to the original Esaki-Tsu result[1] in the zero-temperature limit (so the ratio of Bessel functions goes to one) and when we choose $\gamma_v=\gamma_\varepsilon\equiv 1/\tau$. In this limit, it is easy to see that $\partial j/\partial E_0<0$ for $(eaE_0\tau/\hbar)>1$, so that there is NDC in this regime. Experimentally, both the NDC effect in SSL (Ref. 4) and the effect of thermal saturation of miniband transport in a SSL,[27] due to the dependence of the equilibrium electron energy $\varepsilon_0^{(T)}$ [cf. Eq. (5)] on temperature, have been observed. In this regard, it is interesting to note that the generalization of the formula of Esaki and Tsu to finite temperature and to $\gamma_v\neq\gamma_\varepsilon$ describes with reasonable accuracy the stationary transport properties of a SSL, even in the case when the energy of the external field and the thermal energy of the electrons are comparable to the miniband width, and the quasiclassical description becomes *a priori* inadequate.[5]

We have considered these two special cases in the absence of the self-consistent field, i.e., $E_{\rm sc}(t)\equiv 0$. Importantly, if we include $E_{\rm sc}(t)$, we again find Bloch oscillations (albeit *not* simple sinusoidal motion) in the case of no relaxation effects, and the NDC for the steady-state current-voltage characteristic when relaxation effects are included. We do not present these results in detail here,[28] as they are not essential to our present study.

To prepare for our study of the time-varying external field case, including $E_{\rm sc}(t)$, we introduce some scalings of the variables in Eq. (3), for these will both simplify the analysis and make apparent an important analogy with the nonlinear dynamics in optical systems.

We introduce the variables

$$v=\frac{2\hbar}{\Delta a}V,\quad w=\frac{\varepsilon-\Delta/2}{\Delta/2},\quad w_0=\frac{\varepsilon_0-\Delta/2}{\Delta/2}. \tag{7}$$

$$E=\frac{ea}{\hbar}E_{\rm sc}+\omega_s\cos\Omega t,\quad \omega_s=\frac{dE_0}{\hbar},\quad d=ea. \tag{8}$$

In these variables, Eqs. (3) become

$$\dot v=Ew-\gamma_v v, \tag{9a}$$

$$\dot w=-Ev-\gamma_\varepsilon(w-w_0), \tag{9b}$$

$$\dot E=\omega_E^2 v-\alpha E+f(t), \tag{9c}$$

where

$$f(t)=\alpha\omega_s\cos\Omega t-\omega_s\Omega\sin\,\Omega t\quad\text{and}$$

$$\omega_E=\left[\frac{2\pi e^2Na^2\Delta}{\hbar^2}\right]^{1/2}. \tag{10}$$

It follows from Eq. (5) that $w_0^{(T)}=2\varepsilon_0^{(T)}/\Delta-1$. The variable w in Eq. (7) has a simple physical interpretation: namely, it is the electron's energy measured from the middle of the miniband and normalized by the half-width of the miniband. Hence the value $w=-1$ corresponds to the bottom of the miniband, and $w=1$ corresponds to the upper edge of the miniband. The field E is the total electric field (measured in units of frequency) acting on the electrons. Note that the frequency ω_E is *formally* equal to the frequency of electron plasma oscillations, $\omega_{\rm pl}=[4\pi e^2N/m_0]^{1/2}$, *provided* that m_0 is taken as the effective electron mass at the bottom of the miniband, as given by Eq. (4). For this reason, the corresponding cooperative oscillations of the coupled SSL system were called ''nonlinear plasma oscillations'' by Epshtein.[11] However, since the term ''plasma oscillations'' is usually used in a different context in semiconductors,[2,10] we shall refer to these as ''cooperative oscillations,'' and denote their frequency by ω_E.

The analogy mentioned in Sec. I between the present SSL problem and optical systems helps to clarify this point further. If we consider the variable w in Eqs. (9) to be the population difference and v the polarization, then Eqs. (9) are equivalent to the coupled Maxwell-Bloch (CMB) system, taking into account the external field (see, for example, Ref. 29). Recall that the CMB equations describe the dynamics of two-level atoms placed in a single-mode cavity, and interacting with the cavity field via a dipole interaction. The width of the SSL miniband $(\Delta/\hbar)$ is equivalent to the transition frequency (ω_0) of the two-level atom. The value ea of the SSL is the transition dipole moment (d) in the CMB case. Finally, the analog of the frequency ω_E defined by Eq. (10) is the so-called ''cooperative frequency'' $\omega_c \equiv (2\pi\omega_0 d^2 N/\hbar^2)^{1/2}$.[30] The physical interpretation of this cooperative frequency is the frequency of the slow resonant exchange of energy between the N two-level atoms and the field in the cavity, as first described by the Dicke model.[30] In the balance equations describing the SSL system [Eqs. (9)], the miniband is treated as initially empty. When the N electrons are injected, the assumption that they are distributed with spatially homogeneous density means that the ''populated'' miniband becomes analogous to an optical system consisting of an ensemble of two-level atoms with density N in the Dicke model. Our self-consistent field is analogous to the cavity field, and the cooperative oscillations of the Dicke type appear due to the coupling of the electrons in the miniband to the self-consistent field. The relaxation parameter α in our SSL equations plays the role of the finite quality factor of the cavity in the optical system. Finally, the Stark frequency $\omega_s = eaE_0/\hbar$ is equivalent to the Rabi frequency $\omega_R = dE_0/\hbar$.

Equations (9) are also similar to the CMB equations describing the dynamics of a laser with an injected signal,[31] or a bistable system in the framework of the Bonifacio-Lugiato model.[29,32] However, there are important differences between Eqs. (9) and the optical analog systems. First, the CMB equations are derived for the field and the polarization envelopes; hence the variables v and E in the CMB equations are generally complex. Second, the form of the external force $f(t)$ that perturbs the cavity mode is different in the CMB equations. Nonetheless, the structural similarities and the well-known results that under certain conditions transitions to chaos take place in the bistable devices[29,32] and also in lasers both with[33] and without injected signals[34,35] suggest that one should expect transitions to chaotic dynamics in the SSL plus field interaction problem. In Sec. III we will show that this is indeed the case.

III. CHAOTIC DYNAMICS IN SEMICONDUCTOR SUPERLATTICES

Exploring the chaotic dynamics in Eqs. (9) is a formidable task, for we have in effect a four-dimensional dynamical system — three independent variables (v, w, and E) plus the explicit external time dependence — involving six parameters (γ_v, γ_ε, α, ω_E, ω_s, and Ω). Fortunately, we can obtain some guidance concerning the ''interesting'' regions of parameter and state space by noting that our equations reduce, in two different limits, to two well-known systems which exhibit chaos. We discuss these two limits in the ensuing two subsections.

A. Lorenz equation limit

When the external ac field is absent [$f(t) \equiv 0$], Eqs. (9) are equivalent to the well-known Lorenz model.[36] Although one can derive this equivalence directly, it can also be seen immediately from our optical analogy: namely, for $f(t) \equiv 0$, Eqs. (9) coincide with the CMB equations describing a single-mode homogeneously broadened laser at exact resonance between the cavity mode and two-level atomic transition,[34] and it has been shown by Haken[35] that CMB equations can be reduced to the Lorenz model by a simple transformation of variables.

Translating the necessary conditions for instability and the transition to chaos in the Lorenz model[34–36] into our notation, we find that these conditions can be written as

$$\alpha > \gamma_v + \gamma_\varepsilon \tag{11a}$$

and

$$w_0 > \frac{\gamma_v \alpha^2}{\omega_E^2} \frac{(\alpha/\gamma_v + \gamma_\varepsilon/\gamma_v + 3)}{(\alpha - \gamma_\varepsilon - \gamma_v)}. \tag{11b}$$

The condition in Eq. (11b) requires that the value w_0 corresponding to the electron's equilibrium energy should be larger then some critical value $w_0^{(\mathrm{cr})} > 0$. From Eq. (5), we see that even at high temperatures ($T \to \infty$) the equilibrium value $w_0^{(T)} \to -0$. Hence we find the interesting result that in the Lorenz limit ($f(t) \equiv 0$), the necessary conditions (11b) for the transition to chaos can not be satisfied in the SSL system; to obtain chaos in the SSL system, we require additional driving ($f(t) \neq 0$).

B. Damped, driven Josephson junction limit

When $\gamma_v = \gamma_\varepsilon = 0$, Eqs. (8a) and (8b) immediately imply the existence of a constant of motion: namely, the length of the pseudospin vector, which we can, without loss of generality, scale to 1, so that

$$v^2(t) + w^2(t) = 1. \tag{12}$$

We can incorporate this conservation law explicitly and consistently into the dynamics by introducing the change of variables

$$v = -\sin\theta, \quad w = -\cos\theta, \quad \theta = \int_0^t dt' E(t'). \tag{13}$$

From these definitions (and noting that $\dot{\theta} = E$), one sees that Eqs. (9a) and (9b) are automatically satisfied, and that Eq. (9c) becomes

$$\ddot{\theta} + \alpha\dot{\theta} + \omega_E^2 \sin\theta = \omega_s(\alpha \cos\Omega t - \Omega \sin\Omega t). \tag{14}$$

Introducing $\phi_0 = \tan^{-1}(\Omega/\alpha)$, we can recast Eq. (14) into the form

$$\ddot{\theta} + \alpha\dot{\theta} + \omega_E^2 \sin\theta = \rho \cos(\Omega t + \phi_0), \tag{15}$$

where $\rho=\omega_s\sqrt{\alpha^2+\Omega^2}$. This is the canonical form of the damped, (ac) driven pendulum equation, widely studied in chaotic dynamics both in its own right and as a model for a damped, driven Josephson junction.[37] We shall exploit this connection further in our detailed analysis of the numerical results below.

In the limit of no dissipation whatever — $\alpha=0$ as well as γ_v and γ_ε — the SSL plus field system reduces to the Hamiltonian system which we studied in Ref. 18 for a range of physically reasonable initial conditions; interested readers should consult this reference for details. Here we simply remark that this nondissipative chaos in the SSL plus field system has its own optical analogy, involving the generalized semiclassical Tavis-Cummings (TC) model, which describes the dynamics of two-level atoms in a single-mode high-quality cavity, interacting with self-consistent and external fields.[38] Details of the chaotic dynamics in the TC model can be found in Refs. 38 and 39.

It is well known that both Eq. (15) and its undamped counterpart contain chaotic dynamics.[40] In terms of our parameters, the parameter region in which strong chaos is expected is $\omega_E\sim\omega_s\sim\Omega$; in Sec. III C, we shall use this information as the starting point for our study of chaos in the full SSL plus field problem.

C. Dissipative chaos in the presence of an external time-periodic field

We now consider the general case, in which $f(t)$, γ_v, γ_ε, and α are all nonzero. The structure of the Eqs. (9) suggests that we take ω_E as the scale of (inverse) time, and thus the natural damping parameters that occur in the rescaled equations are the dimensionless quantities γ_v/ω_E, $\gamma_\varepsilon/\omega_E$, and α/ω_E. Since there is considerable uncertainty in the individual values of the phenomenological damping parameters, we will study a broad range of values of these parameters: $0\leqslant\gamma_v/\omega_E$, $\gamma_\varepsilon/\omega_E\leqslant 0.2$, and $0\leqslant\alpha/\omega_E\leqslant 0.2$. Since there are as yet no direct measurements of the cooperative oscillations or their damping, we have chosen conservative upper damping limits inferred from recent results determining that the ratio of the line width of the *plasma* oscillations to their frequency can be as large as 2×10^{-1}.[41,42] For initial conditions, we take $E(0)=\omega_s$, $v(0)=0$, and $w(0)=-1$, corresponding to the initially unexcited SSL just being struck by the incident EM radiation. For our numerics we used a fifth-order Runge-Kutta algorithm incorporating adaptive step size, accuracy checking, and Cash-Karp optimized parameters.

The variable most directly related to experimental observables is the average electron velocity v. Accordingly, we will focus on the various different behaviors of v that follow from the solutions of Eqs. (9) and the regions in which they occur. In Fig. 1 we show the two basic types of behavior for v observed in our simulations. Fig. 1(a) shows behavior in the ''regular'' region, in which the velocity varies periodically. In Fig. 1(a), the basic frequency is just the fundamental frequency of the external EM field with a longer period modulation (caused by the nonlinearity of the equations) superimposed. The ''locking'' of the oscillations of the electron's velocity to the fundamental frequency of the external field is referred to as ''1:1 mode-locking behavior'' in the

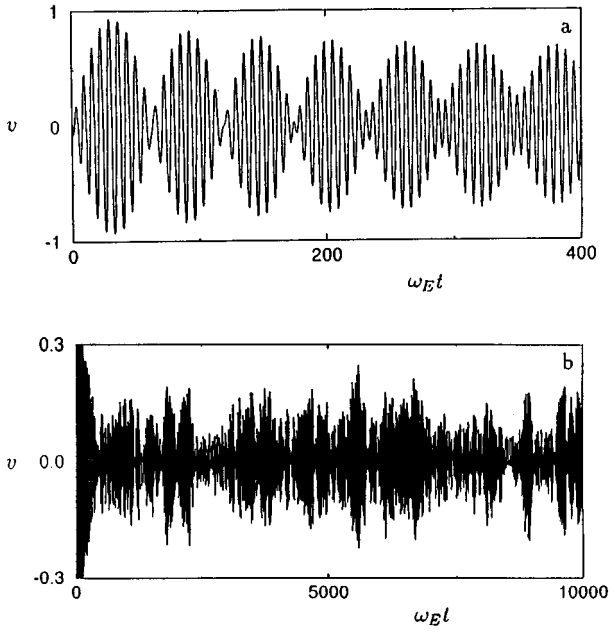

FIG. 1. Dependence of the electron's average velocity on time for $E(0)=\omega_s$, $v(0)=0$, and $w(0)=-1$: (a) ''regular'' (periodic) dynamics (for $\omega_s/\omega_E=0.1$, $\Omega/\omega_E=1$); (b) chaotic dynamics (for $\omega_s/\omega_E=1.6$, $\Omega/\omega_E=0.2$).

Josephson junction literature[37] and in related studies of coupled oscillators. Figure 1(b) shows a typical behavior in the ''chaotic'' region, in which the velocity varies erratically and with no apparent periodicity for as long as we observe it; this is ''stationary chaos,'' and is the behavior in which we are most interested. Within the region of parameters in which chaos is observed, we also observe a behavior which exhibits characteristics of both regular and stationary chaotic motion: namely, a (typically long) interval of ''erratic,'' aperiodic motion, followed by a near vanishing of the oscillations and then a locking into a periodic motion; this *transient chaos* is illustrated in Fig. 2. Importantly, the time at which the transient chaos disappears, $t_{\rm tr}$ is a sensitive function of the numerics, especially the level of accuracy demanded of the numerical integrator. This is commonly encountered in simulations of chaotic systems.

In the regions of transient chaos, the asymptotic state is periodic. Visual inspection of Fig. 2(b) shows that for these parameter values the final period is also the fundamental of the external period, but we have also observed (for other parameter values) locking to different subharmonics of this period. The general case of locking into periods other than the fundamental period of the external drive is well known from general results in nonlinear dynamics, and is exhibited explicitly by the damped, driven Josephson junction.[37] Given our present focus on establishing the possibility of chaotic motion in the SSL system, we shall not present further details here.[28]

To quantify these three types of behavior systematically, we used standard dynamical systems tests: for each set of parameters, we calculated the maximum Lyapunov exponent λ using the method described in Ref. 43 and determined the power spectrum (using a fast Fourier transform algorithm) for each of the velocity plots. In Fig. 3 we show the typical

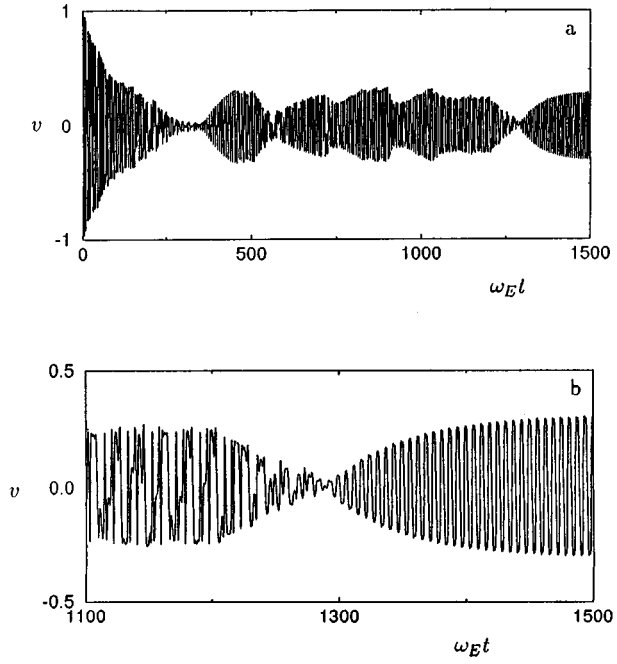

FIG. 2. Dependence of the electron's average velocity v on time for transient chaos ($\gamma_v/\omega_E=\gamma_\varepsilon v/\omega_E=0.01$, $\alpha/\omega_E=10^{-3}$, $\omega_s/\omega_E=1.5$, and $\Omega/\omega_E=1$): (a) long-time behavior; (b) transition to the laminar phase.

behavior of the maximal Lyapunov exponent for the cases of regular motion and chaotic motion. With the standard definitions and calculational procedures,[43] the Lyapunov exponent will vary in time, eventually converging to the value

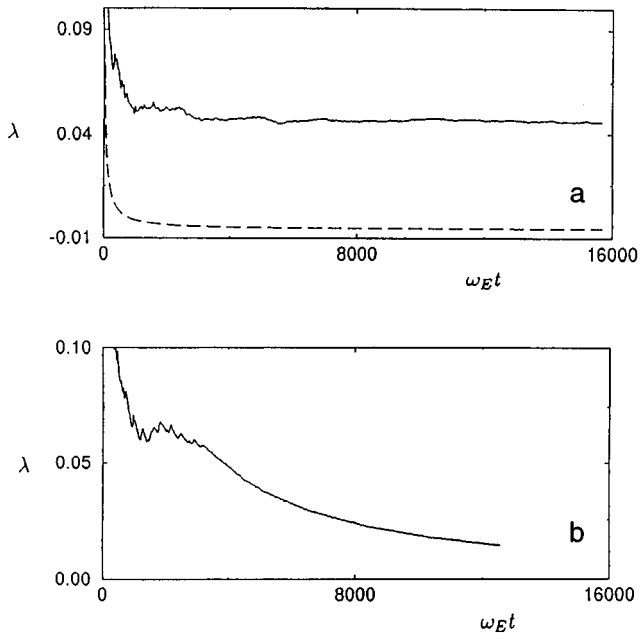

FIG. 3. Dependence of the maximal Lyapunov exponent on time: (a) for chaotic motion [solid curve; the parameters are the same as in Fig. 1(b)]; and for periodic motion (dashed curve; for $\omega_s/\omega_E=1.3$, $\Omega/\omega_E=0.2$); (b) for the transient chaos shown in Fig. 2.

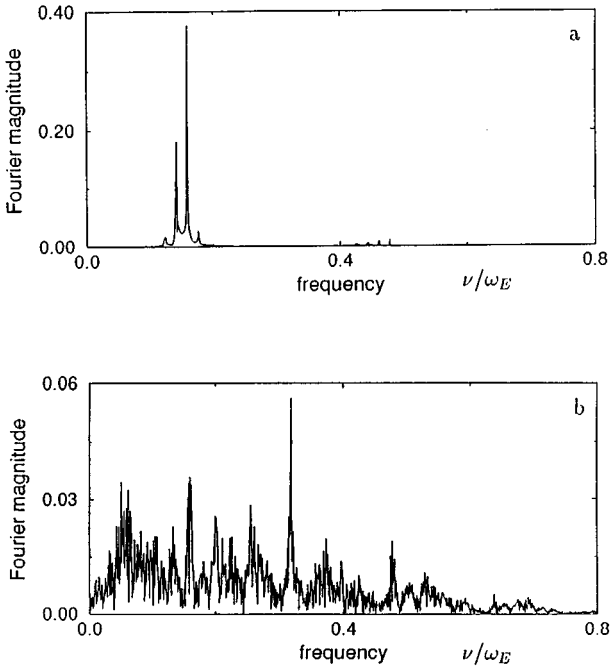

FIG. 4. Power spectrum vs frequency for the electron's velocity v: (a) regular motion [parameters are the same as in Fig. 1(a)]; (b) transient chaos (parameters are the same as in Fig. 2). For the case of the transient chaos, the frequency spectrum was calculated only for the turbulent phase.

reflecting the underlying long-time dynamics. We see from Fig. 3 that, for the chaotic motion, the asymptotic value of λ is greater than zero, as it should be, whereas for the periodic behavior it is less than zero. For the parameter values chosen in Fig. 3(a), this asymptotic value is only slightly negative, consistent with the fairly weak dissipation for these values of the parameters. For the case of transient chaos, shown in Fig. 3(b), the Lyapunov exponent decays to its final value only very slowly. In Fig. 4 we show typical power spectra for periodic and chaotic motion. Note the expected appearance of a broad power spectrum in the chaotic case, in contrast to the isolated peaks associated with the periodic evolution.

The best overview of the qualitative nature — chaotic versus periodic — of the behavior of the system is provided by a two-dimensional plot showing, for fixed values of γ_v, γ_ε, and α, the locations of the regions with *positive* values of the Lyapunov exponent as functions of the two parameters of the external field, ω_s and Ω, measured in units of ω_E. This sort of plot provides a clear visual presentation of the chaotic regions, and has been used very effectively in studies of chaos in the damped, driven Josephson junction.[37] Here it will allow us readily to see how various types and amounts of damping effect the extent of chaos in our system.

In Fig. 5 we present the first of the plots of λ vs ω_s and Ω. For purposes of comparison with Ref. 37, we have chosen the parameters to correspond to the case of the Josephson junction ($\gamma_v=\gamma_\varepsilon=0$), and have produced a plot of the λ in the $(\rho-\Omega)$ plane instead of the $(\omega_s-\Omega)$ plane; again, the plots are in units of ω_E. As stressed above, this is not a physically plausible set of parameters for real a SSL because it neglects crucial velocity and energy dissipation effects, but

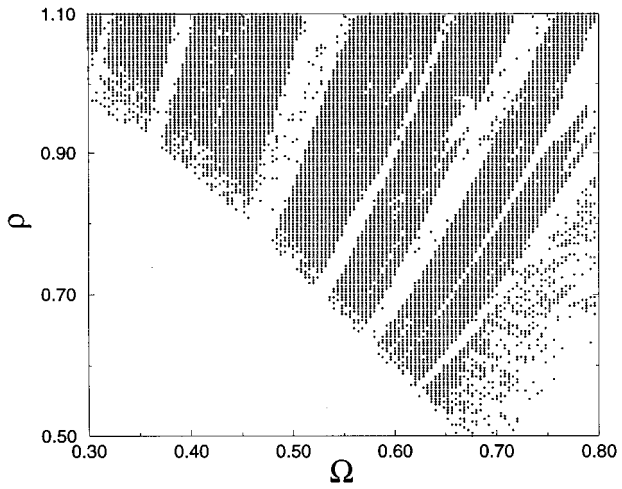

FIG. 5. A plot of the regions of periodic (white, $\lambda<0$) and chaotic (symbols, $\lambda>0$) motion in the ρ-Ω plane; the values of the damping constants are $\gamma_v=\gamma_\varepsilon=0$ and $\alpha=0.2$, corresponding to the case of the damped, driven Josephson junction studied in Ref. 37. In this and all subsequent figures, all parameters are measured in units of ω_E.

it does provide a convincing test of our numerics, for direct comparison shows that our results (plotted here with $\alpha/\omega_E=0.2$) are in full agreement with those of Ref. 37 as far as concerns the structure of the chaotic regions; further, although we shall not present the details of the harmonics in the periodic regions because they are not germane to our current discussion, we have also found[28] good agreement with Ref. 37 for the periodic regions. Qualitatively, Fig. 5 shows us the triangularly shaped southern extremity of a large chaotic region (which extends upwards for toward larger values of ρ). From the left-hand boundary of the chaotic region (indicated by the symbols) many different periodic channels (indicated by the white regions) cut into the chaotic region; these channels correspond to the different subharmonic periodic lockings observed in simulations of Josephson junctions.

Turning to parameter values more relevant to SSL's, we show in Figs. 6(a)–6(d) the evolution of the chaotic region as the values of the damping parameters are varied over a wide range. In Fig. 6(a) we begin from the limit of fairly small dissipation ($\gamma_v=\gamma_\varepsilon=0.01$ and $\alpha=0.001$). Note that in Fig. 6 and henceforth, all damping parameters are scaled in units of ω_E. In this case, the ''order-chaos'' boundary is very close to the boundary found in Ref. 18 for the Hamiltonian model; given the fairly small values of the relaxation parameters, this is perhaps not terribly surprising. Further, the chaotic region is very solid, with few of the channels observed in Fig. 5 (or in subsequent figures discussed below).

In Fig. 6(b) all relaxation rates have been increased by a factor of 10 (so that $\gamma_v=\gamma_\varepsilon=0.1$, and $\alpha=0.01$). The chaotic region in this case shows considerably more structure, with a number of channels cutting into the left boundary, while the right boundary has receded substantially, leaving a smaller, isolated separate region of chaos. Increasing the damping still more reduces the chaotic region, first to the narrow main region plus small isolated regions in Fig. 6(c) and then to the two tiny isolated regions of chaos in Fig. 6(d). These figures make clear that while the size and shape of the chaotic region are strong functions of damping, chaos is expected to occur for a wide range of values. In particular, for the expected range of the velocity and energy damping parameters, $0.01\leqslant\gamma_v,\gamma_\varepsilon\leqslant0.1$ (Refs. 41 and 42) found in the highest quality SSL's, chaos appears likely to occur over a substantial range of parameters.

Let us comment on several qualitative features of the chaotic regions in Fig. 6, beginning with Fig. 6(a). Perhaps the most striking qualitative feature here is the clear distinction between the left boundary of the chaotic region, which appears very sharply defined, and the right boundary, which is substantially more diffuse.

An enlargement of the right boundary, shown in Fig. 7(a), indicates fractal-like behavior, since zooming in on the region does not decrease its ramified structure. Although this structure is theoretically interesting, the experimental consequences are likely to be limited. First, in this region, many of the positive Lyapunov exponents are nearly zero, and are thus sensitive to small effects from the numerics. It is thus difficult to be certain of the boundaries between periodic and chaotic behavior. To illustrate the sensitivity to a cutoff on the size of λ, in Fig. 7(b) we show the same enlargement of the right boundary with the constraint that $\lambda>0.01$. The difference between Figs. 7(a) and 7(b) is readily apparent. Second, since, as shown in Fig. 3(b) and discussed above, the Lyapunov exponents can sometimes relax very slowly to their asymptotic values — leading to regions of ''transient chaos''— determining the true asymptotic value of λ can be difficult. Indeed, the precise boundary in Fig. 7(a) is very sensitive to the details of the numerical code, including discretization effects, and a different code would likely not reproduce it exactly. Particularly if there is a fractal boundary[44] for the actual differential equation system, this effect is to be expected. In contrast, the left boundary in Fig. 6(a) is very sharply defined: the negative exponents jump suddenly to large positive ones as the chaotic region is entered.

Our interpretation of these features can be described qualitatively in terms of familiar concepts from dynamical systems. Recall that in exhaustive studies of general nonlinear dissipative dynamical systems, one fixes the parameters and varies the initial conditions, searching for all the ''attractors'' and determining the shape of each basin of attraction in the space of initial conditions. Typically there is more than one attractor in the system, and the boundaries between the different basins of attraction can be smooth or fractal.[44] After determining completely the attractor structure for one set of parameters, one then moves on to another set, and does a similar search through the space of initial conditions. In our study, which is intended to be illustrative of the possible existence of chaos in SSL's (rather than exhaustive), we have for simplicity *fixed* the initial conditions and varied the parameters. As a consequence, if there are multiple attractors, as we change parameters for fixed initial conditions, we can pass from one basin of attraction another, and the structure of the basin boundaries —fractal or smooth— will be reflected in the plots of the chaotic regions as in Figs. 5–7. More extensive numerical studies, which we will report elsewhere,[28] confirm this explanation.

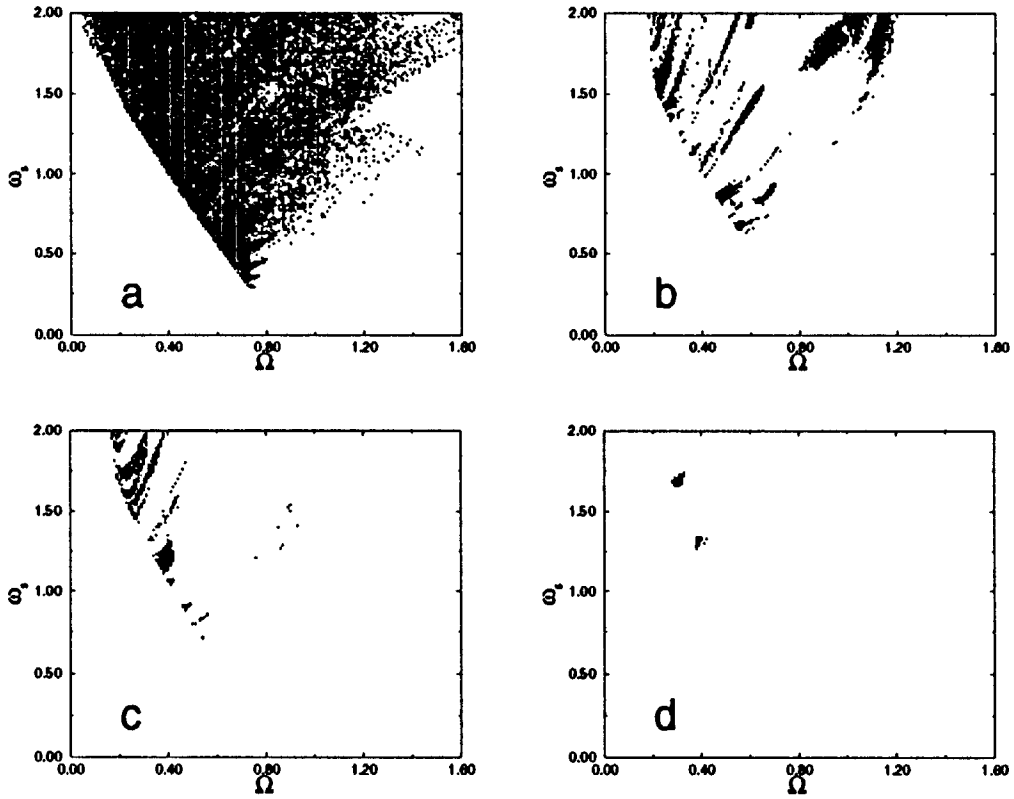

FIG. 6. Plots showing the regions of periodic (white, $\lambda<0$) and chaotic (symbols, $\lambda>0$) motion in the ω_s-Ω plane for four different values of the damping parameters: (a) $\gamma_v=\gamma_\varepsilon=0.01$, $\alpha=0.001$; (b) $\gamma_v=\gamma_\varepsilon=0.1$, $\alpha=0.01$; (c) $\gamma_v=\gamma_\varepsilon=0.1$, $\alpha=0.05$; and (d) $\gamma_v=\gamma_\varepsilon=0.2$, $\alpha=0$.

In Figs. 6(b) and 6(c), the size of the chaotic region decreases successively, and the periodic channels become apparent. These figures — particularly Fig. 6(b) — interpolate nicely between the case of the damped, driven Josephson junction (Fig. 5) and the case of Fig. 6(a). The presence of these periodic channels within the chaotic region raises the possibility of observing not only chaos in SSL's but also mode lockings to various subharmonics of the driving frequency, and we are currently investigating this possibility.[28]

In real SSL's, one typically has $\gamma_v \gg \gamma_\varepsilon$. In our previous discussion, we have for simplicity considered only the case $\gamma_v=\gamma_\varepsilon$. Figure 8 illustrates the extent of the chaotic region when $\gamma_v=0.1 \gg \gamma_\varepsilon=0.02$; this reduction in the chaotic region for unequal damping is typical.[28] Restricting ourselves to the physically relevant regime in which $\gamma_v>\gamma_\varepsilon$, we can summarize our data qualitatively by saying the region of chaos is largest when γ_ε is roughly equal to γ_v or α, whichever is larger.

Finally, we note that for simplicity in all the above results we worked at zero temperature. From Eq. (5), we see that this corresponds to $\varepsilon_0=0$ ($w_0=-1$). For $\Omega/\omega_E=1$ and for various values of ω_s/ω_E, we investigated the influence of the temperature effects on the transition to chaos. When T was varied from helium to the room temperature, keeping all other parameters fixed, we found no qualitative changes in the nonlinear dynamics within our phenomenological balance equation model. Quantitative details of the temperature dependence will be presented elsewhere.[28]

IV. SUMMARY, DISCUSSION, AND CONCLUSION

We have considered the influence of an ac electric field on the motion of ballistic electrons in a miniband of a semiconductor superlattice. Within a phenomenological balance equation approach, we established that accounting for collective effects (via a self-consistent field) leads to the possibility of chaotic dynamics. Our numerical and analytic results suggest that for a transition to chaos one must satisfy the following conditions: (i) the frequency of the ac field (Ω) should be close to the characteristic frequency of the collective electron motion (ω_E) in the SSL; (ii) at the same time, the frequency of the ac field should be close to the Stark frequency $\omega_s=eaE_0/\hbar$, which is determined by the *amplitude* of the external field; and (iii) the relaxation rates of the electron's energy and momentum should not be too large ($\gamma/\omega_E \lesssim 0.2$).

Importantly, it appears possible to achieve these conditions in real SSL's, now or in the near future. For typical superlattices ($a\sim10^{-6}$ cm, $\Delta\sim10^{-2}$ eV, and $N\sim10^{14}$ cm^{-3}), the characteristic frequency of the cooperative oscillations lies in the THz domain ($\omega_E\approx1.5\times10^{12}$ s^{-1}).[9,41,45] If an ac field with amplitude ~1 kV/cm is applied to an SSL with period $a\sim10^{-6}$ cm, the Stark frequency also lies in the THz domain. Thus the frequency constraints can likely be achieved.

Although the damping effects and relaxation rates are much less well known, there nonetheless appears to be rea-

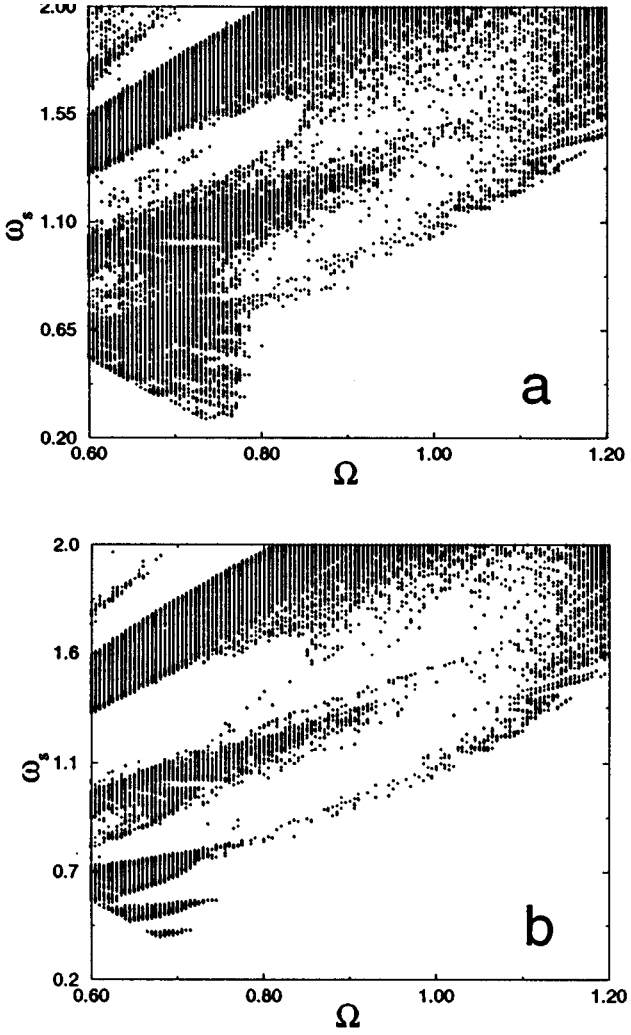

FIG. 7. Plots showing an enlargement of the right boundary of the chaotic region for the parameters $\gamma_v=\gamma_\varepsilon=0.05, \alpha=0.01$ as determined by requiring that (a) $\lambda>0.001$ and (b) $\lambda>0.01$.

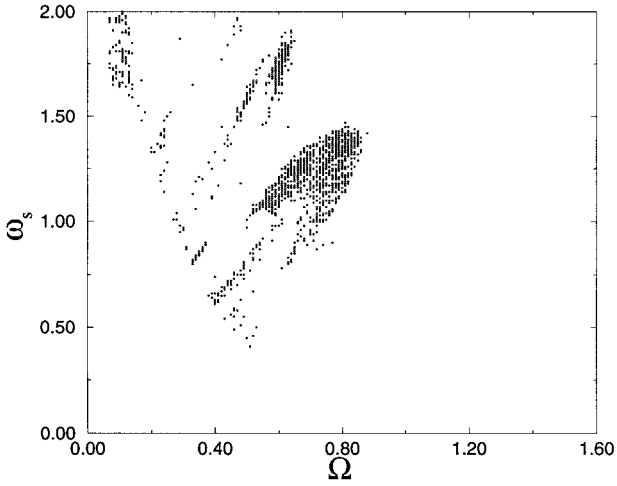

FIG. 8. Plots showing the chaotic region in the case in which the elastic scattering time is considerably larger than the inelastic scattering time. The parameters are $\gamma_v=0.1, \gamma_\varepsilon=0.02$, and $\alpha=0.01$.

son for some optimism. As we have indicated above, standard estimates of the relevant relaxation constants for the plasma oscillations give values in the range of $(10^{-1}-10^{-2})\omega_{\rm pl}$.[41,42] That the damping is more likely near the larger end of this range is suggested by the observation that the phase relaxation rate even in a good quantum well is the relatively rapid $\tau_v \simeq 3.5\times 10^{-12}$ s,[46] which corresponds to near-THz frequencies. For a modulation-doped superlattice, τ_v is almost certain to be shorter, since the electrons may scatter from dopant impurities not present in the remotely doped quantum wells. Hence, the damping effects in current SSL's may be nearer the high end of our range of parameters. One intriguing possibility for producing SSL's with lower relaxation rates involves ''implanting'' the superlattices within parabolic quantum wells;[47] in this manner, one could hope to achieve the low damping levels of good quantum wells and avoid the damping effects associated with modulational doping. A separate complication concerning damping effects is that energy relaxation processes in both wells and superlattices also involve many distinct processes. From quantum-well studies,[46] we expect that the energy relaxation cannot be described *quantitatively* by a single constant γ_ϵ. Although it would clearly be possible to introduce energy-dependent relaxation rates into our phenomenological equations, without more detailed experimental guidance as to the form of this dependence, it is premature to incorporate such an additional complication. Given the relatively large range of relaxation parameters over which our phenomenological model predicts chaotic behavior for the SSL plus field system, the present uncertainties in the exact level and nature of damping in these systems are not cause for undue concern.

Thus, we believe that by applying an ac field of order ~ 1 kV/cm with frequency of the order of several THz to a SSL, one should be able to satisfy the requirements for transition to deterministic chaos. For instance, in the recent experiment[7] first studying the influence of a THz field on the stationary electron transport properties in a SSL, the experimental conditions were close to those required for the observation of chaos in our model system. Further, continuing progress in both the fabrication of heterostructures with high carrier mobility and in the design of powerful sources of THz radiation[46] suggests that the experimental observation of the deterministic chaos in a SSL plus field interaction may be close at hand.

An essential question for experimentalists is how to recognize the underlying chaotic electron dynamics in the observables measured in a real experiment. As the controversy over the observation of Bloch oscillations suggests, this may not be a simple matter. In large part, it will depend on precisely how the experiment is configured and instrumented. At this stage, and without considering in detail the configuration of a particular proposed experiment, we can most appropriately give a somewhat general answer. If chaos is present, we expect a complex, aperiodic behavior for the average velocity, and hence the average current. Given the high frequencies involved, it seems unlikely that one could measure this directly in the time domain. However, in the presence of an additional dc voltage, to create nonzero mean ''drift'' in this average velocity, the oscillatory chaotic com-

ponent would appear as a substantial additional source of apparent ''noise'' in drift velocity and that this additional noise would appear suddenly as one crossed the threshold to chaos, particularly for the parameter regime corresponding to the left boundary of the chaotic region. Specifically, if one measured the power spectrum associated with the current, one would observe the same substantial increase in the broadband ''noise'' component that we see in Fig. 4. In an experiment on a resistively shunted Josephson tunnel junction [related to the model in our Eq. (15)], precisely such a dramatic increase in experimental noise was observed when the parameters of the experimental system were moved through the transition to chaos.[48] A second option for detecting chaos would involve sampling the current at given time intervals and using the ''phase-space reconstruction'' techniques[49] to create a geometrical image of the underlying attractor. For regular motion, the attractor will be a simple periodic structure; for chaotic motion, it will be a ''strange attractor.'' The details of this approach are described in the context of an experiment involving germanium photoconductors in Ref. 50. Additional details about experimental techniques for detecting chaotic motion in semiconductor structures are described in Ref. 46.

Apart from the most central issue of experimental verification of the existence of chaos, there are a number of open theoretical issues which merit further study. First, our model is applicable in the limit of *miniband* transport for the electrons and assumes a spatially homogeneous structure for the EM field. One could ask whether these assumptions are crucial to the possible existence of chaos in SSL's. A recent study by Bulashenko and Bonilla[51] suggests strongly that this is not the case. Focusing on the resonant-tunneling regime and considering the possibility of high-field domain effects (nonhomogeneity in space), these authors also find possible chaotic behavior. Since the crossover between the resonant-tunneling and miniband regimes of transport depends on many experimental and material parameters, some more controllable than others, and remains a complicated problem for theorists, it is important to note that these essentially complementary studies, taken together, suggest that chaos is a robust phenomenon in SSL's. Second, there is a clear need to understand the extent to which our phenomenological balance equation approach correctly captures the physics contained in more microscopic considerations, such as the full Boltzmann equation or an approach based on Wigner distribution function,[20] and on the anticipated region of validity for any miniband-based approach. Although there has been some recent progress on the former issue,[24] there remains much to be done on both problems.

Let us conclude with a brief speculative comment related to the possible consequences and relevance of chaotic behavior in SSL's. Based on the earlier experience of studying chaos in semiconductor devices used for infrared radiation detection,[50] mapping out the boundary of chaos experimentally is important to reliable use of the devices in the ''normal'' regime. However, recent developments in ''controlling chaos''[52] suggest that one might actually deliberately choose to drive the SSL into a chaotic regime, in order to take advantage of the myriad possible behaviors there for device applications. Alternatively, using methods of chaotic control, one may be able to suppress the onset of chaos, as was recently done in an experimental laser system.[53] Chaotic control and reduction of chaos are also likely to be important for future nanofabricated semiconductor integrated circuits, where the expected chip densities will be of the order $10^9/\mathrm{cm}^2$.[2] At such densities, the devices actually form a *lateral surface superlattices*, and device-device interactions can generate both cooperative effects and additional instabilities.[54] In any case, a large number of exciting experimental and device-related problems remain.

ACKNOWLEDGMENTS

It is a pleasure to thank Mark Sherwin for many valuable discussions on experimental aspects of SSL's. We also gratefully acknowledge useful comments from Feo Kusmarsev, Jesper Myqind, Mads Sorensen, and Stephanos Venakides. K.N.A. and G.P.B. thank The Center for Nonlinear Studies, Los Alamos National Laboratory, and the Department of Physics at The University of Illinois at Urbana-Champaign, for their hospitality. This work was partially supported by grants from INTAS (94-2058) and INTAS-RFBR (657I96) and by Linkage Grant No. 93-1602 from the NATO Special Programme Panel on Nanotechnology. E.H.C. thanks the U.S. Department of Education for support by a GAANN Fellowship (DE-P200A40532), and M.C.C. thanks the U.S.-NSF for support under its REU program (NSF Grant No. PHYS93-22320).

[1] L. Esaki and R. Tsu, IBM J. Res. Dev. **14**, 61 (1970).

[2] For useful summaries of technological issues and references to the literature related to the fabrication of nanoscale electronic devices, see D.K. Ferry, Y. Takagaki, and J.-R. Zhou, Jpn. J. Appl. Phys. **33**, 873 (1994); D.K. Ferry and H.L. Grubin, *Solid State Physics, Vol. 49, Advances in Research and Applications*, edited by H. Ehrenreich and F. Spaepen (Academic, New York, 1995).

[3] *Negative Differential Resistance and Instabilities in 2D Semiconductors*, edited by N. Balkan, B. K. Ridley and A. J. Vickers, Vol. 307 of *NATO Advanced Study Institute, Series B: Physics* (Plenum, New York, 1993).

[4] A. Sibille, J. F. Palmier, H. Wang, and F. Mollot, Phys. Rev. Lett. **64**, 52 (1990); F. Beltram, F. Capasso, D. L. Sivco, A.L. Hutchinson, S.-N. G. Chu, and A.Y. Cho, *ibid.* **64**, 3167 (1990); H. T. Grahm, K. von Klitzing, K. Ploog, and G. H. Döhler, Phys. Rev. B **43**, 12 094 (1991); C. Minot, H. Le Person, J. F. Palmier, and F. Mollot, *ibid.* **47**, 10 024 (1993); C. Minot, H. Le Person, J. F. Palmier, and J. C. Harmand, in *Ultrafast Phenomena in Semiconductors*, edited by D. K. Ferry and H. M. van Driel [Proc. SPIE **2142**, 326 (1994)].

[5] A. Sibille, J. F. Palmier, M. Hadjazi, H. Wang, G. Etemadi, E. Dutisseuil and F. Mollot, Superlatt. Microstruct. **13**, 247 (1993).

[6] F. Capasso and S. Datta, Phys. Today **43**(2), 74 (1990); L. L. Chang and Leo Esaki, *ibid.* **45**(10), 36 (1992); E. E. Mendez and G. Bastard, *ibid.* **46**(6), 34 (1993).

[7] A. A. Ignatov, E. Schomburg, K. F. Renk, W. Schatz, J. F. Palmier and F. Mollot, Ann. Phys. **3**, 137 (1994).

[8] P. S. S. Guimaraes, Giran J. Keay, Jann P. Kaminski, S. J. Allen, Jr., P. F. Hopkins, A. C. Gossard, L. T. Florez, and J. P. Harbison, Phys. Rev. Lett. **70**, 3792 (1993); B. J. Keay, S. J. Allen, Jr., J. Galán, J. P. Kaminski, K. L. Campman, A. C. Gossard, U. Bhattacharya, and M. J. W. Rodwell, *ibid.* **75**, 4098 (1995); B. J. Keay, S. Zeuner, S. J. Allen, Jr., K. D. Maranowski, A. C. Gossard, U. Bhattacharya, and M. J. W. Rodwell, *ibid.* **75**, 4102 (1995).

[9] E. M. Epshtein, Fiz. Tverd. Tela (Leningrad) **19**, 3456 (1977) [Sov. Phys. Solid State **19**, 2020 (1977)].

[10] L. B. Vatova, Fiz. Tverd. Tela (Leningrad) **15**, 2468 (1973) [Sov. Phys. Solid State **15**, 1639 (1974)].

[11] E. M. Epshtein, Fiz. Tekh. Polupruvodn. **11**, 1386 (1977) [Sov. Phys. Semicond. **11**, 814 (1977)].

[12] E. M. Epshtein, Fiz. Tekh. Polupruvodn. **12**, 985 (1978) [Sov. Phys. Semicond. **12**, 583 (1978)].

[13] F. G. Bass, V. V. Konotop, and A. P. Panchekha, Pis'ma Zh. Éksp. Teor. Fiz. **48**, 106 (1988) [JETP Lett. **48**, 114 (1988)]; Zh. Éksp. Teor. Fiz. **96**, 1869 (1989) [Sov. Phys. JETP **69**, 1055 (1989)]; F. G. Bass and A. P. Panchekha, *ibid.* **99**, 1711 (1991) [*ibid.* **72**, 955 (1991)].

[14] A. A. Ignatov, K. F. Renk, and E. P. Dodin, Phys. Rev. Lett. **70**, 1996 (1993).

[15] Martin Holthaus, Phys. Rev. Lett. **69**, 351 (1992).

[16] F. G. Bass and A. P. Tetervov, Phys. Rep. **140**, 237 (1986).

[17] F. G. Bass and L. B. Vatova, Phys. Rep. **241**, 219 (1994).

[18] K. N. Alekseev, G. P. Berman, and D. K. Campbell, Phys. Lett. A **193**, 54 (1994).

[19] E. Schöll and A. Wacker, in *Nonlinear Dynamics and Pattern Formation in Semiconductors and Devices*, edited by F. J. Niedernostheide, Springer Proceedings in Physics Vol. 79 (Springer, New York, 1994).

[20] J.-R. Zhou and D.K. Ferry, IEEE Trans. Electron Dev. **39**, 473 (1992).

[21] R. A. Suris and B. S. Shchamkhalova, Fiz. Tekh. Polupruvodn. **18**, 1178 (1984) [Sov. Phys. Semicond. **18**, 738 (1984)]; F. G. Bass and E. A. Rubinstein, Fiz. Tverd. Tela (Leningrad) **19**, 1379 (1977) [Sov. Phys. Solid State **19**, 800 (1977)].

[22] A. A. Ignatov and V. I. Shashkin, Phys. Lett. A **94**, 169 (1983); A. A. Ignatov, E. P. Dodin, and V. I. Shashkin, Mod. Phys. Lett. B **5**, 1087 (1991).

[23] X. L. Lei, N. J. M. Horing, and H. L. Cui, Phys. Rev. Lett. **66**, 3277 (1991).

[24] X. L. Lei, J. Phys. Condens. Matter **4**, 9367 (1992); X. L. Lei, N. J. M. Horing, and H. L. Cui, *ibid.* **4**, 9375 (1992); X. L. Lei, *ibid.* **4**, L659 (1992); **5**, L43 (1993).

[25] J. R. Barker and D. K. Ferry, Solid-State Electron. **23**, 519 (1980); **23**, 531 (1980); **23**, 545 (1980); N. C. Kluksdahl, A. M. Kriman, and D. K. Ferry, Phys. Rev. B **39**, 7720 (1989); J.-R. Zhou and D. K. Ferry, IEEE Trans. Electron Dev. **40**, 421 (1993); T. Yamada, J.-R. Zhou, H. Miyata, and D. K. Ferry, *ibid.* **41**, 1513 (1994).

[26] J. Feldmann, K. Leo, J. Shah, D. A. B. Miller, J. E. Cunningham, T. Meier, G. von Plessen, A. Schulze, P. Thomas, and S. Schmitt-Rink, Phys. Rev. B **46**, 7252 (1992); K. Leo, P. H. Bolivar, F. Brüggemann, R. Schwedler, and K. Köhler, Solid State Commun. **84**, 943 (1992).

[27] G. Brozak, M. Helm, F. DeRosa, C. H. Perry, M. Koza, R. Bhat, and S. J. Allen, Jr., Phys. Rev. Lett. **64**, 3163 (1990).

[28] E. H. Cannon, M. Cargo, D. K. Campbell, G. P. Berman, and K. Alekseev (unpublished).

[29] H. M. Gibbs, *Optical Bistability: Controlling Light with Light* (Academic, New York, 1985).

[30] R. H. Dicke, Phys. Rev. **93**, 99 (1954).

[31] N. B. Abraham, L. A. Lugiato, and L. M. Narducci, J. Opt. Soc. Am. B **2**, 7 (1985).

[32] V. G. Benza and S. W. Koch, Phys. Rev. A **35**, 174 (1987).

[33] L. A. Lugiato, L. M. Narducci, D. K. Bandy, and C. A. Pennise, Opt. Commun. **46**, 64 (1983); F. T. Arecchi, G. L. Lippi, G. P. Puccioni, and J. R. Tredicce, *ibid.* **51**, 308 (1984); J. R. Tredicce, F. T. Arecchi, G. L. Lippi, and G. P. Puccioni, J. Opt. Soc. Am. B **2**, 173 (1985); D. K. Bandy, L. M. Narducci, and L. A. Lugiato, *ibid.* **2**, 148 (1985).

[34] H. Haken, *Light, Vol. 2: Laser Light Dynamics* (North-Holland, Amsterdam, 1985).

[35] H. Haken, Phys. Lett. A **53**, 77 (1975).

[36] E. N. Lorenz, J. Atmos. Sci. **20**, 130 (1963); for a detailed study of the Lorenz equations over a wide range in parameter space, see C. A. Sparrow, *The Lorenz Equations: Bifurcations, Chaos, and Strange Attractors* (Springer-Verlag, New York, 1982).

[37] B. A. Huberman, J. P. Crutchfield, and N. H. Packard, Appl. Phys. Lett. **37**, 750 (1980); N. F. Pedersen and A. Davidson, *ibid.* **39**, 830 (1980).

[38] K. N. Alekseev and G. P. Berman, Zh. Éksp. Teor. Fiz. **94**, 49 (1988) [Sov. Phys. JETP **67**, 1762 (1988)].

[39] K. N. Alekseev and G. P. Berman, Zh. Éksp. Teor. Fiz **92**, 1985 (1987) [Sov. Phys. JETP **65**, 1115 (1987)]; D. Holm and G. Kovačič, Physica D **56**, 270 (1992).

[40] B. V. Chirikov, Phys. Rep. **52**, 263 (1979); A. J. Lichtenberg and M. A. Lieberman, *Regular and Stochastic Motion* (Springer-Verlag, New York, 1983).

[41] J. J. Quinn and J. S. Carberry, IEEE Trans. Plasma Sci. **PS-15**, 394 (1987).

[42] R. E. Camley and D. L. Mills, Phys. Rev. B **29**, 1695 (1984); A. C. Sharma and A. K. Sood, J. Phys. Condens. Matter **6**, 1553 (1994).

[43] A. Wolf, J. B. Swift, H. L. Swinney, and J. A. Vastano, Physica **16D**, 285 (1985).

[44] C. Grebogi, E. Ott, and J. A. Yorke, Science **238**, 632 (1987).

[45] S. Perkowitz, *Optical Characterization of Semiconductors: Infrared, Raman, and Photoluminescence Spectroscopy* (Academic, New York, 1993).

[46] M. S. Sherwin, in *Quantum Chaos: Between Order and Disorder*, edited by G. Casati and B.V. Chirikov (Cambridge University Press, New York, 1995), pp. 209–234, and (private communications).

[47] K. L. Campman, M. Sundaram, S. J. Allen, Jr., and A. C. Gossard, Superlatt. Microstruct. **15**, 141 (1994).

[48] R. F. Miracky, J. Clarke, and R. J. Koch, Phys. Rev. Lett. **50**, 856 (1983); K. Wiesenfeld, E. Knobloch, R. F. Miracky, and J. Clarke, Phys. Rev. A **29**, 2102 (1984).

[49] N. H. Packard, J. P. Crutchfield, J. D. Farmer, and R. S. Shaw, Phys. Rev. Lett. **45**, 712 (1980).

[50] R. M. Westervelt, E. G. Gwinn, and S. W. Teitsworth, Nucl. Phys. B (Proc. Suppl.) **2**, 37 (1987); S. W. Teitsworth and R. M. Westervelt, Phys. Rev. Lett. **56**, 516 (1986); E. G. Gwinn and R. M. Westervelt, *ibid.* **59**, 157 (1987).

[51] O. M. Bulashenko and L. L. Bonilla, Phys. Rev. B **52**, 7849 (1995).

[52] For recent reviews, see T. Shinbrot, C. Grebogi, E. Ott, and J. A.

Yorke, Nature **363**, 411 (1993); L. R. Keefe, Phys. Fluids A **5**, 931 (1993).

[53] Z. Gillis, C. Iwata, R. Roy, I. B. Schwartz, and I. Triandaf, Phys. Rev. Lett. **69**, 3169 (1992).

[54] D. K. Ferry, in *The Physics of Submicron Semiconductor Devices*, edited by H. L. Grubin, D. K. Ferry, and C. Jacoboni, Vol. 180 of *NATO Advanced Study Institute, Series B: Physics* (Plenum, New York, 1988), p. 503; and in *Granular Nanoelectronics*, edited by D. K. Ferry, J. R. Barker, and C. Jacoboni, Vol. 251 of *NATO Advanced Study Institute, Series B: Physics* (Plenum, New York, 1991), p. 1.